Title: Adsorption behavior of methylene blue on glycerol based carbon materials

Authors: Apurva A. Narvekar, J.B. Fernandes, S.G. Tilve

PII: S2213-3437(18)30088-5
DOI: https://doi.org/10.1016/j.jece.2018.02.016
Reference: JECE 2208

To appear in:

Received date: 24-10-2017
Revised date: 8-2-2018
Accepted date: 11-2-2018

Please cite this article as: Apurva A.Narvekar, J.B.Fernandes, S.G.Tilve, Adsorption behavior of methylene blue on glycerol based carbon materials, Journal of Environmental Chemical Engineering https://doi.org/10.1016/j.jece.2018.02.016

Adsorption behavior of methylene blue on glycerol based carbon materials

Apurva A. Narvekar, J.B. Fernandes*, S.G.Tilve

Department of Chemistry, Taleigao Plateau, Goa University, Goa – 403206, India.

Corresponding author e-mail address: jbfx@rediffmail.com

Graphical abstract

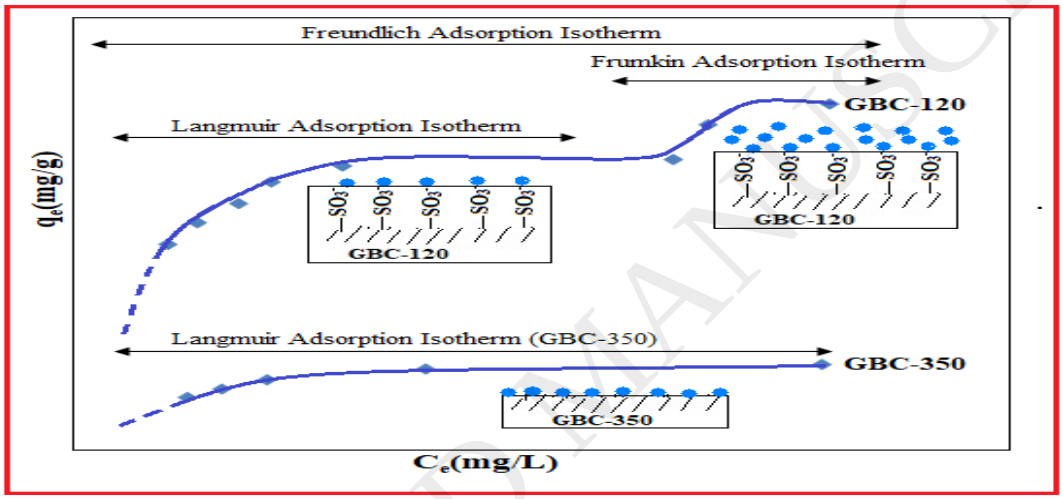

Highlights

- First report of methylene blue adsorption on glycerol based carbons.
- GBC-120 (SO_3H), surface area 21 m^2/g, multilayer adsorption capacity > 1000 mg/g
- GBC-350, 464 m^2/g, gave much lower adsorption ~ 130 mg/g, due to loss of SO_3H function.
- GBC-120 and GBC-350 followed second order adsorption kinetics.

Abstract

In the present investigation a glycerol based carbon was synthesized by partial carbonization of glycerol using concentrated H_2SO_4 in the molar ratio 1:4. The carbonized material was further treated at 120 ^oC and 350 ^oC to obtain the carbons GBC-120 and GBC-350 respectively. The samples were characterized by XRD, ir, thermal analysis (TG-DTG-DTA), pzc measurements; SEM and BET surface area analysis. The TGA showed a gradual weight loss up to about 800 ^oC. The adsorption studies were carried out using

methylene blue as a model adsorbate. The BET surface area of GBC-120 and GBC-350 were determined to be 21 and 464 $m^2 g^{-1}$. The GBC-120 gave maximum adsorption capacity with nearly 100 % dye removal efficiency using 8-10 milligrams of the adsorbent powder, when the dye concentration was 25μg mL^{-1}. It showed Type I adsorption isotherm profile at lower concentration range and the data could be readily fitted into Langmuir adsorption model. At higher concentration the adsorption data showed a better fit for Frumkin adsorption model. The adsorption generally increased with temperature and showed a favorable free energy change. The GBC-350 showed comparatively less adsorption and but the data could also be fitted in Langmuir adsorption profile. Investigation of adsorption kinetics revealed better fit with pseudo second order kinetic model for both GBC-120 and GBC-350. GBC-120 due to presence of SO_3H surface functionality showed a high adsorption capacity ~ 1050 mg g^{-1} which is significantly higher than the literature values.

Key words: glycerol, sulphonyl, adsorption, kinetics, methylene blue

1. Introduction

There is a continuing interest in developing newer methods of synthesis of carbon materials as adsorbents and catalysts. In recent times, increasing attention is given to develop functionalized carbon materials that could both act as excellent catalysts and also have improved adsorption characteristics [1]. Carbon catalysts with acid functionalities are finding increasing use in organic transformations. A glycerol based carbon (GBC) was recently synthesized by partial carbonization of glycerol using sulfuric acid. This carbon was found to be an effective solid acid catalyst in organic transformations including chemo selective synthesis [2-5]**.** This was due to the presence of acidic functionalities such as SO_3H on its surface. Thus the GBC carbon was found to be advantageous over other carbon catalysts owing to its ease of synthesis, efficiency and comparative stability.

On the other hand activated carbons obtained from different natural sources including nutshells, wood, coconut husk etc. often need appropriate chemical or physical activation in order to get efficient activity. However glycerol as a carbon source is readily available as a byproduct of biodiesel production industry and is thus cost effective. In addition to being used as a catalyst, a glycerol based carbon was also recently synthesized for adsorptive removal of antibiotics from their aqueous solutions [6,7].

Apart from being used as adsorbents and catalysts, carbons are also required as supports for noble metal catalysts such as electrocatalysts in fuel cell reactions. The catalysts used in fuel cells are often platinised carbons such as Pt-C or Pt-Ru/C etc. These carbon supports need to be very pure carbon materials free from any metallic impurities as well as free from any residual chloride or sulphur. Since glycerol is readily available in a pure form, it is amenable towards appropriate synthesis of pure carbon materials of desired properties. Depending upon synthesis conditions, it should also be possible to use glycerol as a raw material to synthesize pure microporous carbon or mesoporous carbon with desired surface functionalities. A series of investigations would thus be required to selectively develop various forms of carbon starting

from glycerol as a raw material and then tailor its properties to make it useful either as an adsorbent or as a catalyst or as a catalyst support or having combination of these characteristics. In the present investigation, a glycerol based carbon is synthesized and examined for its adsorption behavior towards removal of methylene blue. The knowledge gained here is expected to be a background information when further studies are undertaken in development of suitable glycerol based carbon materials. Since methylene blue is also a well known pollutant associated with effluents from textile industry, the present investigation will throw light not only on surface characteristics of the glycerol based carbon but also on its efficacy in mitigating pollutants by adsorption.

The activated carbons play a crucial role in mitigating pollutants such as dyes, pharmaceuticals, surfactants, heavy metal ions etc. by adsorption from industrial waste waters [8-12].
The dyeing process in the textile industry leads to release of approximately 10 – 15 % dyes into the environment. The effluents from these industries thus carry a large number of dyes and other additives which are added during the coloring process [13]. Due to their high water solubility they get readily transferred through water bodies. They may also undergo degradation to form products that are highly toxic [14]. Thus removal of dyes from the water bodies is important as they are harmful for living beings. A widely used cationic dye in different industries is methylene blue which is known to be carcinogenic.

Adsorption by activated carbons is an important process for removal of pollutants particularly dyes and metal ions from industrial waste waters. Adsorption is a very effective separation technique in terms of initial cost, simplicity of design, ease of operation and insensitive to toxic substances. It is a tertiary technology during waste water treatment for adsorption of micropollutants, as well as to remove colour and odor [15]. The efficiency of removal by adsorption from solution depends upon the nature of dyes (cationic or anionic dyes), pH of adsorbate solution, pzc of the adsorbent and its surface functionalities, as well as surface area and porosity of the adsorbent. The use of different adsorbents like clay, silica materials, zeolite and activated carbons for removal of methylene blue (MB) has been extensively studied and is recently reviewed [16]. A variety of adsorbents have been designed depending upon the type of adsorbates to be removed. Activated carbons are generally more effective adsorbents for removal of high molecular weight compounds particularly those with low water solubility. However activated carbons with surface functionalities are efficient for adsorbing a wider range of organic pollutants such as dyes and pharmaceuticals.

Zhang et al., [17] have examined the comparative adsorption of two cationic dyes (Rhodamine B and Methylene blue) by milled sugarcane bagasse which gave an adsorption capacity of 31 mg g^{-1}. Similarly Xiong et al., [18] studied the adsorption of methylene blue on titanate nanotubes and maximum adsorption capacity of 133 mg g^{-1} was reported. Among all the described adsorbents in literature, the ability of activated carbons is eminent for adsorption of dyes due to its ease of availability and economic feasibility. It is one of the most widely used adsorbent as compared to

all other materials. Adsorption of methylene blue onto activated carbon produced from steam activated bituminous coal was reported with maximum adsorption capacity of 580 mg g^{-1} at equilibrium [19]. Further, adsorption from aqueous solutions onto carbon nanotubes was also studied wherein monolayer adsorption capacity of 132 mg g^{-1} was observed [20]. Recently a high adsorption capacity for methylene blue (714 mg g^{-1}) was reported when birnessite type manganese dioxide in presence of diatomite, was used as an adsorbent for the removal of MB in alkaline solution (pH 11). It was however not considered favorable for regeneration and reuse [21]. The microwave-induced H_2SO_4 treated activated carbon obtained from rice agricultural wastes was also used for methylene blue sorption and maximum adsorption capacity of 62.5 mg g^{-1} at initial pH of 7 is reported [22]. In general carbon materials obtained from various biomass sources showed adsorption capacity from methylene blue in the range 100 - 600 mg g^{-1}[23-30].

The nature of interaction between the adsorbate molecules and the adsorbent can be understood from the adsorption isotherms. An adsorption isotherm is a plot which relates the amount of substance adsorbed to the equilibrium concentration of the adsorbate molecules in the solution at a specified temperature. The amount adsorbed depends on the nature of adsorbate and adsorbent which in turn affect the shape of adsorption isotherm profile. The data is usually investigated in terms of different adsorption isotherm models which include, Langmuir, Freundlich, Frumkin adsorption isotherms. These are considered in the present investigation. The Langmuir Isotherm assumes that adsorption is of monolayer and all the active sites on the adsorbent surface are equivalent in energy. Freundlich adsorption isotherm explains the multilayer adsorption behavior. For understanding interaction between adsorbed molecules, the applicability of Frumkin adsorption isotherm is generally investigated. The description of adsorption isotherms and kinetic models [31-36] used in this work are briefly summarized in Table 1.

2. **Experimental**

2.1 Chemicals and materials

Glycerol (GR) was purchased from Molychem (India), Sulphuric acid (AR) was obtained from RUNA (India), Methylene blue (dye content > 96.0 %.) was purchased from S D Fine-Chem Limited (India). Double distilled water was used during the adsorption studies.

2.2 Synthesis and Characterization of glycerol based carbon

The sulphonated glycerol based carbon was synthesized by dehydration of glycerol using sulphuric acid in the molar ratio (*1*: *4*) [2, 6]. Thus 25 mL (Density = 1.84 g mL^{-1}) of sulphuric acid was added drop wise to 10 g of glycerol under continuous stirring over a period of 25 min (approximately at the rate of 1 mL min^{-1}). During the process, glycerol was taken in a 500 mL beaker and kept on hot plate magnetic stirrer. The sulphuric acid was added from a overhead reservoir. As the temperature was increased from ambient temperature to 180 ^oC, the clear solution gradually became a brown viscous mass. The temperature of the product was continued to be maintained at 180 ^oC for another 20 minutes until the evolution of the gases was completed.

The black mass was then filtered and washed with hot water until the washings were neutral. The product was designated as GBC-120. The yield of GBC-120 (carbon-SO_3H) was 0.467 gram per gram of glycerol used. The details of preparing GBC-120 and GBC-350 are summarized in Scheme 1.

Characterization

The carbon samples were characterized by XRD on a Rigaku Ultima IV diffractometer using Cu-Kα radiation of wavelength of 1.5419 Å. Thermal analysis was carried out using TG-DTA analyzer (NETZSCH STA 409 PC) in N_2 atmosphere at a heating rate of 10 $^oC\ min^{-1}$. The infrared spectra were recorded in KBr dispersion, using Shimadzu IR Prestige-21 FTIR spectrophotometer from 4000 - 400 cm^{-1}. The surface area was obtained by multipoint BET method and BJH pore size distribution analysis using Quantachrome® ASiQwin™ - Automated Gas Sorption system. The morphology of carbon samples was determined with environmental scanning electron microscope (Ouanta FEG 250). To determine pHpzc of the carbon samples, various solutions having pH values ranging from 2-10 were prepared. The pH values were adjusted by drop wise addition of HCl (0.02 M) or NaOH (0.02 M) to 50 mL solutions of 0.01 M NaCl. 0.15 g of carbon was then added to each of these solutions, which were then stirred for 24 hours. The final pH of the solutions was then measured. A graph of final pH v/s initial pH was plotted and the pHpzc was obtained from the intersection point.

2.3 Adsorption

2.3.1 Effect of adsorbent dosage

2, 4, 6, 8, 10 mg of GBC-120 were each taken in conical flasks containing 100 mL of 5 μg mL^{-1} solution of methylene blue. The adsorption was carried out at pH 4.7. The flasks were kept for shaking overnight (~15 hours) and the amount adsorbed in each case was determined.

2.3.2 Effect of initial Methylene blue concentration

The dye concentration were varied from 10-50 μg mL^{-1}. The adsorption was carried out using 2 mg of GBC-120. The adsorption was allowed to take place overnight (~15 hours). The adsorption was carried out at pH 4.7.

2.3.3 Effect of initial pH

2 mg of GBC-120 was contacted with 50 mL of 50 μg mL^{-1} of methylene blue at different pH (2.6-9.6). The flasks were kept for shaking for 2 hours and then the amount of methylene blue adsorbed was determined.

2.3.4 Effect of contact time and determination of adsorption equilibrium

The time required to establish equilibrium between the concentration of methylene blue adsorbed and its concentration in the solution was determined. Thus 20 mg of the previously dried carbon sample was added to known concentration (50 μg mL^{-1}) of methylene blue (pH=7). The progress

of adsorption was monitored by taking out 1.0 mL aliquots of the solution at various predetermined time intervals until the equilibrium is reached. The data was interpreted in terms of relevant kinetic models.

2.3.5 Adsorption Isotherms

The adsorption isotherms of GBC-120 and GBC-350 carbons were determined at ambient temperature by equilibriating various concentrations of methylene blue with a know amount of the carbons (~ 2 mg). All the solutions were allowed to equilibriate at 25 ^{o}C at predetermined equilibriation times. The equilibrium concentrations were calculated by measuring the absorbance of methylene blue solution in each case. The data was then fitted in various adsorption isotherm and kinetic models.

3. Results and Discussion

3.1 Characterization techniques

XRD and Thermal analysis

The synthesized glycerol based carbon was characterized by XRD, thermal analysis and infra-red spectroscopy. Fig.1 gives the XRD profiles of the samples GBC-120 and GBC-350.

Both the samples showed the expected two broad peaks at 2θ around 20 - 24^{o} and 43^{o} which correspond to reflection planes of (002) and (100) respectively [37]. It was observed that the peak at 43^{o} was diffuse for the as prepared GBC-120 sample, due to its comparatively amorphous nature.

Fig. 2 gives thermal analysis profiles of GBC-120 carried out in N_2 atmosphere. The TGA profile (Fig. 2a) shows an initial weight loss of ~ 16.4 % up to 108 ^{o}C, due to loss of physisorbed and hydrogen bonded water. Further weight loss continues till about 800 ^{o}C due to gradual loss of the surface functional groups. The DTA shows a broad endothermic profile in this temperature range with a maximum around 600 ^{o}C. This suggested that the loss of surface functionalities was accompanied with structural rearrangement, resulting in development of porosity in the carbon structure. It can be seen from Fig 2 (b) that the TG-DTG profile of GBC-120 exhibits a broad weight loss between 180 - 700 ^{o}C. This broad range shows three distinct regions. The peak at 220 ^{o}C is considered as characteristic for decomposition of –SO_3H and –COOH groups. A large broad peak between 280 to 460 ^{o}C is due to decomposition of lactones and phenolic groups. And the similar broad peak from 460 to 700 ^{o}C is due to decomposition of carbonyl group. These results are in agreement with a recent report on a similarly prepared carbon based catalyst [38].

Infrared spectral analysis

Fig 3 gives the infrared spectra of GBC-120 carbon and the spectra recorded after subjecting it to various heat treatments between 200 - 800 ^{o}C.

The glycerol based carbon which is known to have -SO_3H groups attached to polycyclic cluster of graphitic rings, shows characteristic absorptions in the infrared region of 1720 – 900 cm^{-1} [39-43]. The corresponding assignments are given in Table 2.

From Fig. 3b, it can be observed that when GBC-120 was heated at varying temperatures above 120 ^{o}C, the intensity of -SO_3H peak at 1044 cm^{-1} decrease. This peak vanished by 300 ^{o}C while the other peaks at 1208 cm^{-1} and 1355 cm^{-1} which are also due to -SO_3H functionality were still +present. Thus the thermal treatment at 300 ^{o}C resulted in partial decomposition of -SO_3H due to dehydroxylation of the adjacent sulphonyl groups. The other peaks at 1593 and 1721 cm^{-1} were due to C = C and C = O groups respectively. The carbonyl peak is a composite peak due to –CHO and –COOH and in agreement with the ir spectra reported earlier [44]. A –CHO functionality was expected as it is known that glycerol in presence of sulphuric acid decomposed via an acrolein type intermediate which has a –CHO group [45]. The peak at 1721 cm^{-1} was present till 700 ^{o}C. It eventually disappeared for the GBC-800 sample when the carbonyl functionalities were finally decomposed. This is supported by the evidence from the thermal analysis profile (Fig. 2) that decomposition of the surface functionalities gets completed around 800 ^{o}C.

Surface area, porosity and SEM

Fig. 4 gives the N_2 adsorption desorption isotherms along with pore size distribution profiles for GBC-120 and GBC-350. A clear hysteresis loop was observed for both the samples. The surface area and porosity values are presented in Table 3 along with SEM data.

It can be seen from Table 3 that GBC-120 with its associated SO_3H functionalities showed a relatively small surface area of about 21 m^2 g^{-1}. On the other hand GBC-350 showed much larger surface area of 464 m^2 g^{-1}. This suggested that the partial decomposition of SO_3H greatly enhances the surface area of the carbon due to greater dispersion of the GBC-350 particles. This is supported by the respective SEM images (Fig. 5) wherein GBC-120 shows larger agglomerates as compared to GBC-350. Further, the increased surface area of GBC-350 exposes its surface porosity resulting in its having much larger pore volume. Thus the pore volume of GBC-350 was 0.099 cm^3 g^{-1} as compared to 0.065 cm^3 g^{-1} for GBC-120 even though both the samples have similar pore radii of around 18.3 Å.

3.2 General adsorption behaviour

The adsorption studies were carried out to investigate the influence of SO_3H groups on the carbon surfaces. The removal efficiency of the methylene blue dye from the solution was calculated using the relation

$$Removal\ (\%) = \frac{C_i\ - C_e}{C_i} \times 100 \qquad (3.1)$$

and equilibrium adsorption was determined using the equation:

$$q_e = \frac{C_i - C_e}{W} \times\ V \qquad (3.2)$$

C_i and C_e are the initial and equilibrium concentrations of the dye in µg mL^{-1} respectively, W is the weight of carbon in g and V is volume of the dye solution in litres.

3.2.1 Effect of adsorbent dosage

The effect of adsorbent dosage was studied by taking methylene blue solution of 25 µg mL^{-1}. 100 mL aliquots of the above solution were equilibrated by stirring with varying quantities of the adsorbents for 15 hours. The resulting adsorption behavior is shown in Fig. 6. It can be seen that the relative percent removal of the dye gradually increased and the adsorption efficiency was nearly 100% with 8-10 mg of the carbon. The adsorption capacity or q_e thus obtained using equation 3.2 was around 300 mg g^{-1} of the carbon. This investigation was carried out at pH 4.7. This was the unadjusted pH value was observed when GBC-120 carbon was stirred in methylene blue solution. Further studies were carried out to investigate the effect of pH on probable enhancement in adsorption.

3.2.2 Effect of initial pH

2 mg of GBC-120 carbon was stirred for 2 hours with 50 mL of methylene blue solution having concentration of 50 µg mL^{-1}. The pH of the solutions were adjusted in the range 2.6-9.6 using either HCl or NaOH. Fig. 7 shows the percent efficiency of methylene blue at various pH values. It can be seen from the Fig.7 that there is low adsorption efficiency at lower pH values and the adsorption tends towards maximum in the pH range 7-9. Therefore the subsequent adsorption studies were carried out at pH around 7.
The adsorption capacity at pH 7 using equation 3.2 was 428 mg g^{-1}.

Adsorption following regeneration: GBC-120 was regenerated by treatment with small amount of concentrated H_2SO_4. Further, 10 mg of the regenerated carbon was treated with 20 mL of methylene blue solution of concentration 50 µg $mL^{-1}$and the pH was adjusted to 7. The adsorption was carried out for 2 hours using the original and regenerated carbons. The amount adsorbed in both the cases was found to be around 419 mg g^{-1}. Thus GBC-120 carbon could be easily regenerated and reused.

3.2.3 Effect of initial methylene blue concentration

Adsorption studies were carried out by equilibriating 2 mg of GBC-120 carbon using 100 mL methylene blue solution having initial concentrations of 10, 20, 30, 40, 50 µg mL^{-1}. The pH of each solution was adjusted to 7. The results are presented in Fig 8. It can be seen from the figure that the mass of 2 mg carbon could completely remove methylene blue solution from its initial concentration of 10 µg mL^{-1}. This was equivalent to an adsorption capacity of 500 mg g^{-1}.

3.2.4 Effect of contact time and determination of adsorption equilibrium

The adsorption was studied by equilibriating 20 mg of carbon with methylene blue solution of concentration 50 µg mL^{-1}. The adsorption was studied in two separate experiments in which the pH of the methylene blue solution was 4.7 and 7.0 respectively. The adsorption was carried out for about 15-20 hours until no further adsorption occurred as evident from constant absorbance of the supernatant solution. The resulting adsorption time profiles are given in Fig. 9.

At pH 4.7, the amount adsorbed gradually increased and became maximum (about 300 mg g^{-1}) after about 13 hours. It is seen in the previous section that adsorption increases with pH. Hence adsorption equilibrium-time profile was also investigated at pH 7.0. It was seen that adsorption increased at relatively faster rate and equilibrium was reached within 7 hours. The amount adsorbed under this condition reached a high value of about 1050 mg g^{-1}. This is noteworthy since the recent literature suggest that maximum adsorption capacity of methylene blue on activated carbon is up to about 580 mg g^{-1} . This high adsorption capacity of GBC-120 is due to its SO_3H functionality. It is shown that when surface functional groups are affected by thermal treatment at 350 ^oC the adsorption capacity significantly drops to 130 mg g^{-1}.

3.3 Adsorption isotherm

An adsorption isotherm is a plot of amount of substance adsorbed per unit mass of adsorbent as a function of various equilibrium concentrations at a specified temperature. Typically an adsorption isotherm falls in one of the six specified categories [46]. Accordingly the plots are classified into Type I, Type II etc. The nature of these plots depends on nature of adsorbate and adsorbent. Further the adsorption is influenced by the surface area, porosity and nature of surface functionalities of the adsorbent. Various mathematical expressions are available to describe the nature of adsorption as described in Table 1. Typical adsorption behavior involves Langmuir adsorption. It corresponds to rapid rise in adsorption as concentration increases, and ends up with a plateau region due to saturation of surface adsorption sites. The Freundlich adsorption isotherm extends to further adsorption beyond saturation due to formation of multilayers.

Fig 10 (a) gives the general adsorption isotherm profile observed in this work for adsorption of MB on GBC-120. It showed Type I adsorption behavior in the lower concentration range. Such a behavior is expected for Langmuir adsorption isotherm. However at higher concentration above 10 µg mL^{-1} of the adsorbate, adsorption suddenly increased suggesting an overall Freundlich type of adsorption behavior.
The general adsorption behavior represented above in Fig 10 (a), the experimental points can be fitted in one or more mathematical descriptions of adsorption isotherm models such as those reviewed in Table 1. Fig. 10 (b-d) gives corresponding plots. The data extracted from these plots is presented in Table 4.

It is clear from Fig. 10 (b) that the data fitted well for Langmuir adsorption isotherm with coefficient of determination R^2 value of 0.93 and value of Xm obtained from the graph was close to the observed value around 750 mg g^{-1}. The low value of Langmuir adsorption constant K is indicative of predominantly Van der Waals type of adsorption. On the other hand Freundlich adsorption 1/n was about 0.22. 1/n which represents intensity of adsorption usually have values between 0 to 1. From the q_e versus C plot (Fig 10 (a)) it is seen that the overall fit is better for Freundlich adsorption isotherm across the full concentration range studied.

However it is seen from Fig.10 (d) that the Frumkin adsorption isotherm fits the experimental data well at higher concentration with coefficient of determination R^2 value of 0.99 with a positive interaction parameter α having a value of 3.9 μg mL^{-1}. This is due to multiple adhesive interactions between the surface SO_3H groups and MB molecules as well as the cohesive attractive interaction between the adsorbed MB multilayers. Evidence for such interactions during adsorption of MB on smectites was reported earlier [47]. Further the high value of α equal to 3.9 is also indicative of lateral interaction between the adsorbate molecules in adjacent layers resulting in greater tendency for desorption or breakdown of the multilayers. This is supported by negative value of β.

3.4 Thermodynamic Studies

The evaluation of thermodynamic parameters following adsorption studies have been recently reviewed [50-53]. Thus the free energy change for the adsorption process and the corresponding Langmuir adsorption constant K_L can be shown to be related by the equation [48, 50]

$$\Delta G^o = -RTlnK_L \qquad (3.3)$$

The Langmuir isotherm with the following form has been commonly used for description of adsorption data at equilibrium [50]

$$q_e = q_{max}\frac{C_eK_L}{C_eK_L+1} \qquad (3.4)$$

in which q_e and q_{max} are the adsorption capacity of adsorbent at equilibrium (mg g^{-1}) and its maximum value, C_e, is the equilibrium concentration of adsorbate in solution (moles L^{-1}),

K_L can be calculated using the equation 3.4 [50]:

$$K_L = \frac{\theta_e}{(1-\theta_e)C_e} \text{ where } \theta_e = \frac{q_e}{q_{max}} \qquad (3.5)$$

Since $\Delta G^o = \Delta H^o - T\Delta S^o$,

it follows that the enthalpy of activation and entropy of activation can be evaluated by using the equation

$$lnK_L = -\frac{\Delta H^o}{R}\frac{1}{T} + \frac{\Delta S^o}{R} \qquad (3.6)$$

Where R is the universal gas constant (8.314 J mol^{-1} K^{-1}) and T is temperature in Kelvin at which adsorption is carried out. Fig. 12 gives a plot of ln K_L v/s 1/T from which the activation parameters are calculated and are given in Table 5.

It is clear from these values that the free energy change becomes progressively more negative suggesting increasing spontaneity in adsorption as the temperature was increased from 289 K to 323 K. The enthalpy of activation for the adsorption process as calculated from the ln K v/s 1/T plot, was 102 KJ mol^{-1}. This confirmed that the formation of the activated complex during adsorption is an endothermic process.

3.5 Adsorption behavior of GBC-350

GBC-350 is formed by partial decomposition of SO_3H groups from GBC-120. When GBC-350 was stirred in methylene blue solution its pH remained close to 6.5. Fig. 13 (a-d) gives the general adsorption isotherm profile and its applicability to various adsorption isotherm models. It showed comparatively low adsorption (~130 mg g^{-1}) which was about 10 times less than that observed for GBC-120.

It can be seen from the Fig. 13 (a) that there was initial rapid rise in adsorption. This was followed by decrease in adsorption till there was saturation of adsorption. Such a behavior is generally observed during monolayer formation. As expected the Langmuir adsorption model fitted the data more appropriately with R^2 value of 0.95 as compared when other adsorption models, Freundlich and Frumkin were used wherein the R^2 values were found to be generally less than 0.9.

Fig. 14 describes the comparative adsorption behavior of GBC-120 and GBC-350. The corresponding equilibriation times in relation to rate of adsorption are given in table 7.

It can be seen from the above Figure that GBC-120 showed rapid adsorption in the beginning till it reached equilibrium at the end of 7 hours. On the other hand, GBC-350, although showed much lower adsorption, its initial rate of adsorption was much higher as evident from the initial slope of 61 mg g^{-1} hr^{-1} as compared to GBC-120 whose initial slope was only 28 mg g^{-1} hr^{-1}. The higher equilibrium adsorption of 1050 mg g^{-1} on GBC-120 was due to presence of large amount of $–SO_3H$ as compared to GBC-350, where some surface functionalities were lost upon the thermal treatment.

The adsorption in GBC-350 was to a large extent completed after about 5 hrs. However complete equilibriation was not reached as there was very small amount of adsorption which occurred very slowly in the time interval of 5-17 hrs. Hence in GBC-350, it can be considered as a two stage adsorption process (i) initial equilibrium due to high surface area (ii) the second slow equilibrium, due to tendency of MB to diffuse into the micropores that were developed in the sample after heating it at 350 ^oC as discussed earlier in 3.1. Accordingly, to evaluate the kinetic parameters, the GBC-350 sample is referred to as GBC-350(I) and GBC-350(II). The corresponding adsorption profile is shown resolved in Fig. 14 (inset)

Further GBC-120 showed relatively low pzc value of 2.0 as compared to that of GBC-350 (3.5). Therefore it is expected that the cationic dye MB will be preferentially adsorbed on GBC-120 having large number of highly acidic sulphonyl groups generally in a dissociated form. The high adsorption in GBC-120 is due to hydrogen bonding between H of $–SO_3H$ functionality on GBC-120 surface and N of the methylene blue dye. A similar hydrogen bonded interaction was proposed during adsorption of methylene blue on iron oxide surface [49]. Further enhanced adsorption is also due to interaction of the cationic dye with the dissociated sulphonyl groups.

3.6 Kinetics of adsorption

The adsorption process from solution generally involves diffusion of the dyes (i) from the bulk solution to near the surface of the adsorbent followed by (ii) diffusion at the boundary layer.

The boundary layer is composed of the surface functionalities of the adsorbent and the pre-adsorbed layer of the adsorbate (MB) as well as the layer of water dipoles. Therefore the boundary layer can offer resistance to diffusion of the adsorbate before the actual adsorption interaction occurs on the available surface sites. (iii) The adsorbate molecules may further diffuse inside the pores of the adsorbent depending upon the nature of adsorbate, adsorbent and equilibriation time [20].
The kinetic data obtained on the GBC samples in the present investigation (Fig. 14) was then fitted in thr first and second order kinetic models (Table 1).

3.6.1. Applicability of pseudo first and pseudo second order kinetic models for GBC-120 and GBC-350.
Fig. 15. gives the pseudo first and pseudo second order kinetic plots for GBC-120, GBC-350(I) and GBC-350(II). The resulting kinetic parameters are summarized in Table 7.

It can be seen from the R^2 values that the GBC-120 (Table 6) showed a relatively better fit for pseudo second order kinetics. This is confirmed by the fact that the value of q_e observed is more closer to the calculated value for all the initial concentrations. On the other hand for GBC-350(I), the R^2 values as well as the observed and calculated q_e values differed widely, 29 and 130 mg g^{-1} respectively for pseudo second order kinetic model. Thus the adsorption process did not follow first as well as pseudo second order kinetics. However GBC-350(II) showed a good fit for pseudo second order adsorption process ($R^2 = 0.999$) as the observed and calculated values of q_e (156 and 139 mg g^{-1}) were quite close. The investigation of the kinetic data was further extended to some of the other well-known kinetic models.

4. Conclusions

A glycerol based carbon (GBC) was synthesized by partial carbonization of glycerol using con H_2SO_4 in the molar ratio 1:4. The carbonized material was further treated at 120 ^oC and 350 ^oC to obtain the carbons GBC-120 and GBC-350 respectively.

The samples were characterized by XRD, ir, thermal analysis (TG-DTG-DTA) and pzc measurements. The TGA showed a gradual weight loss up to about 800 ^oC. The ir spectra of the GBC-120 showed characteristic absorptions due to $–SO_3H$ groups. The ir spectra were also recorded of GBC samples heat treated at various higher temperatures. All the peaks due to surface functionalities were eventually disappeared for the GBC-800 sample, in agreement with thermal analysis wherein the decomposition was complete around this temperature (800 ^oC). The BET surface area of GBC-120 was 21 m^2 g^{-1} while GBC-350 showed much larger surface area of about 464 m^2 g^{-1}.

The adsorption studies were carried out using methylene blue as a model adsorbate. The GBC-120 gave maximum adsorption capacity of 1050 mg g^{-1}. The adsorption efficiency was

observed to be dependent on initial concentration of the dye. There was nearly 100 % dye removal efficiency using 8-10 milligrams of the adsorbent powder, when the dye concentration was 25 μg mL^{-1}.

The GBC-120 showed Type-I adsorption isotherm profile at lower concentration range which obeyed conventional Langmuir adsorption isotherm models. However at higher equilibrium concentration above 10 μg mL^{-1}, the data fits better in Frumkin adsorption model with R^2 value of 0.989 due to large interaction between the adsorbate molecules. The adsorption generally increased with temperature and showed a favorable free energy change.

The GBC-350 showed comparatively less adsorption in spite of its much larger surface area due to loss of SO_3H functionalities

The adsorption data could be fitted in Langmuir adsorption isotherm profile. Investigation of adsorption kinetics revealed better fit with pseudo second order kinetic model for GBC-120 while GBC-350 showed a unique two stage adsorption profile and the data could be better fitted into pseudo second order kinetic model.

This investigation is expected to be an important contribution for further development of glycerol based carbon as an adsorbent, catalyst as well as catalysts support such as in electrocatalysis related to fuel cell where very pure carbon is necessary.

Acknowledgment: We acknowledge University Grant Commission New-Delhi for BSR fellowship F.No.25-1/2014-15 (BSR)/7-09/2007(BSR) to A. A. N.

References

[1] K. V. Raghavan, B. M. Reddy (Eds), Industrial Catalysis and Separations: Innovations for Process Intensification, CRC Press (2014).

[2] B. L. A. Prabhavathi Devi, K. N. Gangadhar, P. S. Sai Prasad, B. Jagannadh and R. B. N. Prasad, A Glycerol-based Carbon Catalysts for the Preparation of Biodiesel, ChemsusChem 2 (2009) 617-620.

[3] K. Ramesh, S. N. Murthy, K. Karnakar, K. H. Reddy, Y. V. D. Nageswar, M. Vijay, B. L. A. Prabhavathi Devi, R. B. N. Prasad, A mild and expeditious synthesis of amides from aldehydes using bio-glycerol-based carbon as a recyclable catalyst, Tetrahedron Lett. 53 (2012) 2636–2638.

[4] K. N. Gangadhar, M. Vijay, R. B. N. Prasad, B. L. A. Prabhavathi Devi, Glycerol-Based Carbon-SO_3H Catalyzed Benign Synthetic Protocol for the Acetylation of Alcohols, Phenols and Amines under Solvent-Free Conditions, Green and Sust. Chem. 3 (2013) 122-128.

[5] C. Ummadisetti, B. N. P. Rachapudi, B. L. A. Prabhavathi Devi, Glycerol-based SO_3H-Carbon Catalyst: A green recyclable catalyst for the chemoselective synthesis of pentaerythritoldiacetals, Eur J Chem 5 (2014) 536-540.

[6] R. S. Ribeiro, A. M. T. Silva, M. T. Pinho, J. L. Figueiredo, J. L. Faria, H. T. Gomesa, Development of glycerol-based metal-free carbon materials for environmental catalytic applications, Catal. Today 240 (2015) 61–66.

[7] S. Álvarez-Torrellas, R. S. Ribeiro, H. T. Gomes, G. Ovejero, J. García, Removal of antibiotic compounds by adsorption using glycerol-based carbon materials, Chem. Eng. J. 296 (2016) 277–288.

[8] Tawfik A. Saleh, Ihsan Budi Rachman, Shaikh A. Ali, Tailoring hydrophobic branch in polyzwitterionic resin for simultaneous capturing of Hg(II) and methylene blue with response surface optimization, Sci. Rep. (2017) DOI:10.1038/s41598-017-04624-6

[9] Tawfik A. Saleh, Nanocomposites of carbon nanotubes/silica nanoparticles and their use for adsorption of Pb(II): from surface properties to sorption mechanism, Desalination and Water Treatment, (2015) 1-15.

[10] Tawfik A. Saleh, Mercury sorption by silica/carbon nanotubes and silica/activated carbon: a comparison study, Journal of Water Supply: Research and Technology-AQUA, (2015) 892-903.

[11] Tawfik A. Saleh, Mustafa Tuzen, Ahmet Sari, Magnetic activated carbon loaded with tungsten oxide nanoparticles for aluminum removal from waters, J. Environ. Chem. Eng. 5 (2017) 2853-2860.

[12] Tawfik A. Saleh, Ahmet Sari, Mustafa Tuzen, Optimization of parameters with experimental design for the adsorption of mercury using polyethylenimine modified-activated carbon, J. Environ. Chem. Eng. 5 (2017) 1079-1088.

[13] Ratna, B. S. Padhi, Pollution due to synthetic dyes toxicity & carcinogenicity studies and remediation, Int. J. Environ. Sci. 3 (2012) 940-955.

[14] E. Rindle, W. J. Troll, Metabolic reduction of benzidine azo dyes to benzidine in the Rhesus monkey, J. Natl. Cancer Inst. 55 (1975) 181-182.

[15] Saleh, M.A.M., Mahmoud, D.K., Karim, W.A.W.A., Idris, A., Cationic and anionic dye adsorption by agricultural solid wastes: a comprehensive review, Desalination 280 (2011) 1–13.

[16] M. A. Mohammed, A. Shitu, A. Ibrahim, Removal of Methylene Blue Using Low Cost Adsorbent: A Review, Res. J. Chem. Sci. 4 (2014) 91-102.

[17] Z. Zhang, I. M. O'Hara, G. A. Kent, W. O. S. Doherty, Comparative Study on adsorption of two cationic dyes by milled sugarcane bagasse, Ind Crops Prod 42 (2013) 41-49.

[18] L. Xiong, Y. Yang, J. Mai, W. Sun, C. Zhang, D. Wei, Q. Chen, J. Ni, Adsorption behavior of methylene blue onto titanate nanotubes, Chem. Eng. J. 156 (2009) 313-320.

[19] E. N. El Qada, S. J. Allen, G. M. Walker, Adsorption of Methylene Blue onto activated carbon produced from steam activated bituminous coal: A study of equilibrium adsorption isotherm, Chem. Eng. J. 124 (2006) 103–110.

[20] Z. Shahryari, A. S. Goharrizi, M. Azadi, Experimental study of methylene blue adsorption from aqueous solution on to carbon nanotubes, Int. J. Water Res. Environ. Eng. 2 (2010) 16-28.

[21] Yu X Zhang, X D Hao, F Li, Z P Diao, Z Y Guo,and J Li, pH-Dependent Degradation of Methylene Blue via Rational-Designed MnO_2 Nanosheet-Decorated Diatomites, Ind. Eng. Chem. Res. 53 (2014) 6966−6977.

[22] Somaye Mashhadi, Hamedreza Javadian, Maryam Ghasemi, Tawfik A. Saleh, Vinod Kumar Gupta, Microwave-induced H_2SO_4 activation of activated carbon derived from rice agricultural wastes for sorption of methylene blue from aqueous solution, Desalination and Water Treatment, (2016) 1-14.

[23] A. A. Spagnoli, D. A. Giannakoudakis, S. Bashkova, Adsorption of methylene blue on cashew nut shell based carbons activated with zinc chloride: The role of surface and structural parameters, Journal of Molecular Liquids 229 (2017) 465–471

[24] B.H. Hameed, A.T.M. Din, A.L. Ahmad, Adsorption of methylene blue onto bamboo-based activated carbon:Kinetics and equilibrium studies, Journal of Hazardous Materials 141 (2007) 819–825

[25] B.H. Hameed, A.L. Ahmad, K.N.A. Latiff, Adsorption of basic dye (methylene blue) onto activated carbon prepared from rattan sawdust, Dyes and Pigments 75 (2007) 143-149

[26] S. Valliammai, Y Subbareddy, K S Nagaraja, B Jeyaraj, Removal of methylene blue by activated carbon of Vigna mungo L and Paspalum scobiculatum:equilibrium, kinetic and thermodynamic studies, Indian J. Chem. Technol. 24 (2017) 134-144.

[27] O. Üner , Ü. Geçgel, Y. Bayrak, Adsorption of Methylene Blue by an Efficient Activated Carbon Prepared from **Citrullus lanatus** Rind: Kinetic, Isotherm, Thermodynamic, and Mechanism Analysis, Water Air Soil Pollut (2016) 227-247.

[28] N. Kannan, M.M. Sundaram, The kinetics and mechanism of methylene blue adsorption on commercial activated carbon (CAC) and indigenously prepared activated, Dyes and Pigments 51 (2001) 25–40

[29] Ü. Geçgel, G. Özcan, and G. Ç. Gürpınar, Removal of Methylene Blue from Aqueous Solution by Activated Carbon Prepared from Pea Shells (Pisum sativum) Journal of Chemistry volume 2013, doi.org/10.1155/2013/614083

[30] A H. Jawad, R A Rashid, M A M Ishak and L D. Wilson, Adsorption of methylene blue onto activated carbon developed from biomass waste by H_2SO_4 activation: kinetic, equilibrium and thermodynamic studies, Desalination and Water treatment, 57 (2016) 25194-25206.

[31] J. H. Potgieter, Adsorption of Methylene blue on activated carbon, J. Chem. Educ. 68 (1991) 349-350.

[32] M. Santhi, P. E. Kumar, Adsorption of basic dye, methylene blue by a novel activated carbon prepared from Typha Angustata, Chem. Sci. Trans. 4 (2015) 389-400.

[33] S. M. Yakout, E. Elsherif, Batch kinetics, isotherm and thermodynamics studies of adsorption of strontium from aqueous solution into low cost rice-straw based carbons, Carbon – Sci. and Tech. (2010) 144-153.

[34] Y. Önal, Kinetics of adsorption of dyes from aqueous solutions using activated carbon prepared from the waste apricot, J. Hazard. Mater. B 137 (2006) 1719-1728.

[35] V. Srivastava, P. Maydannik, Y. C. Sharma, M. Sillanppa, Synthesis and applications of polypyrrole coated tenorite nanoparticles (PPy@TN) for the removal of anionic food dye ‘tartrazine’ and divalent metallic ions viz Pb(II), Cd(II), Zn(II), Co(II), Mn(II) from synthetic wastewater, RSC advances 5 (2015) 80829-80846.

[36] Y. Li, Q. Du, X. Wang, P. Zhang, D. Wang, Z. Wang, Y. Xia, Removal of Lead from aqueous solution by activated carbon prepared from Entermorpha Prolifera by zinc chloride activation, J. Hazard. Mater. 183 (2010) 583-589.

[37] L. Wang, X. Li, J. Ma, Q. Wu, X. Duan, Non-activated, N, S-co-doped Biochar Derived from Banana with Superior Capacitive Properties, Sustain. Energy 2 (2014) 39-43.

[38] M. Gonçalves, R. Rodrigues, T. S. Galhardo, W. A. Carvalho, Highly selective acetalization of glycerol with acetone to solketal over acidic carbon-based catalysts from biodiesel waste, Fuel 181 (2016) 46-54.

[39] J. L. Figueiredo, M. F. R. Pereira, M. M. A. Freitas, J. J. M. Órfão, Modification of surface chemistry of activated carbon, Carbon 37 (1999) 1379 –1389.

[40] R. Fareghi-Alamdari, M. Golestanzadeh, N. Zekri, Z. Mavedatpoor , Multi SO_3H supported on carbon nanotubes: a practical, reusable, and regioselective catalysts for the tert-butylation of p-cresol under solvent-free conditions, J Iran Chem Soc 12 (2015) 12537–549.

[41] P. A. Russo, M. M. Antunes, P. Neves, P. V. Wiper, E. Fazio, F. Neri, F. Barreca, L. Mafra, M. Pillinger, N. Pinna, A. A. Valente, Mesoporous carbon–silica solid acid catalysts for producing useful bio-products within the sugar-platform of biorefineries, Green Chem.16 (2014) 4292–4305.

[42] H. Guo, Y. Lian, L. Yan, X. Qi, R. L. Smith, Cellulose-derived superparamagnetic carbonaceous solid acid catalyst for cellulose hydrolysis in an ionic liquid or aqueous reaction system, Green Chem.15 (2013) 2167-2174.

[43] J. Wang, W. Xu, J. Ren, X. Liu, G. Lu, Y. Wang, Efficient catalytic conversion of fructose into hydroxyethylfurfural by a novel carbon based solid acid, Green Chem.13 (2011) 2678-2681.

[44] L. Na, Z. Jian, Z. Qing-Fang, Quantitative and Qualitative Analyses of Oxygen-containing Surface Functional Groups on Activated Carbon, CHEM J CHINESE U 3 (2012) 548-554.

[45] H. Park, Y. S. Yun, T. Y. Kim, K. R. Lee, J. Baek, J. Yi, Kinetics of the dehydration of glycerol over acid catalysts with an investigation of deactivation mechanism by coke, Appl Catal B; 176–177 (2015) 1–10.

[46] S. Brunauer, L.S. Deming, W.S. Deming, E. Teller, Classification of Adsorption Isotherms, J. Am. Chem. Soc. 62 (1940).

[47] J. Bujdák, M. Janek, J. Madeiová, P. Komadel, Methylene blue interaction with reduced-charged smectites, Clays Clay Miner. 49 (2001) 244-254.

[48] A. S. Özcan, A. Özcan, Adsorption of acid dyes from aqueous solutions onto acid-activated bentonite, J. Colloid Interface Sci. 276 (2004) 39-46.

[49] F. Li, X. Wu, S. Ma, Z. Xu, W. Liu, F. Liu, Adsorption and desorption mechanism of methylene blue removal with Iron-oxide coated porous ceramic filter, J Water Resource Prot 1 (2009) 1-57.

[50] Yu Liu, Is the Free Energy Change of Adsorption Correctly Calculated? J. Chem. Eng. Data 54 (2009) 1981-1985.

[51] Yu Liu, Ya-Juan Liu, Review Biosorption isotherms, kinetics and thermodynamics, Separation and Purification Technology 61 (2008) 229–242

[52] Yu Liu, Hui Xu, Equilibrium, thermodynamics and mechanisms of Ni^{2+} biosorption by aerobic granules, Biochemical Engineering Journal 35 (2007) 174–182.

[53] E. C. Lima, M. A. Adebayo, F. M. Machado, Chapter 3- Kinetics and Equilibrium Models of Adsorption in Carbon Nanomaterials as Adsorbents for Environmental and Biological Applications, C. P. Bergmann, F. M. Machado editors, ISBN 978-3-319-1887-4, Springer (2015) 33-69.

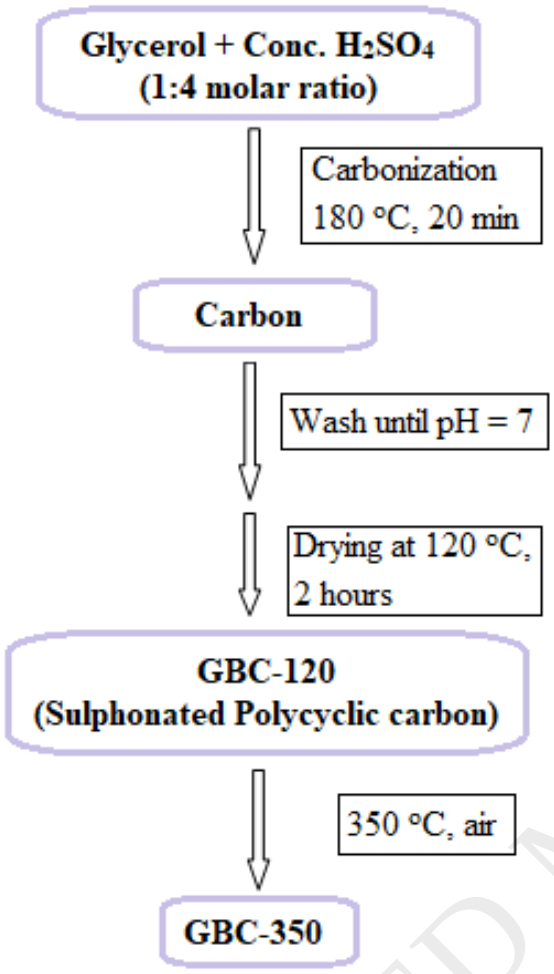

Scheme 1. Flow chart for synthesis of the glycerol based carbons (GBC-120 and GBC-350).

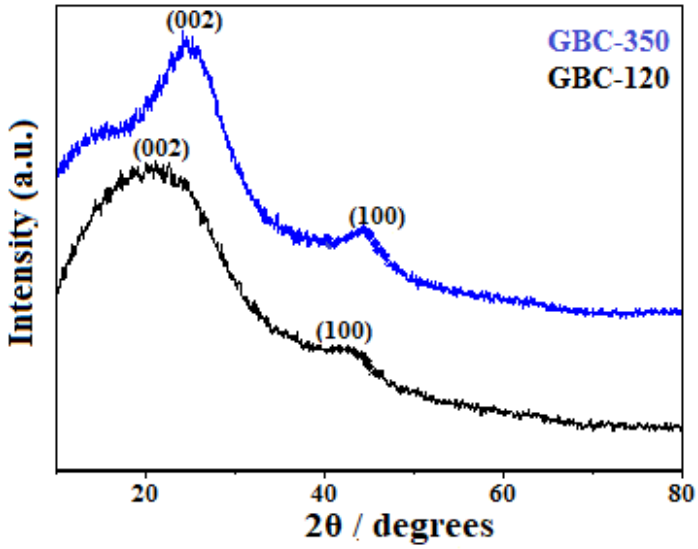

Fig.1. XRD profiles of the glycerol based carbons obtained by treatment of the as prepared carbons at 120 ºC and 350 ºC using Cu-Kα radiation of wavelength of 1.5419 Å.

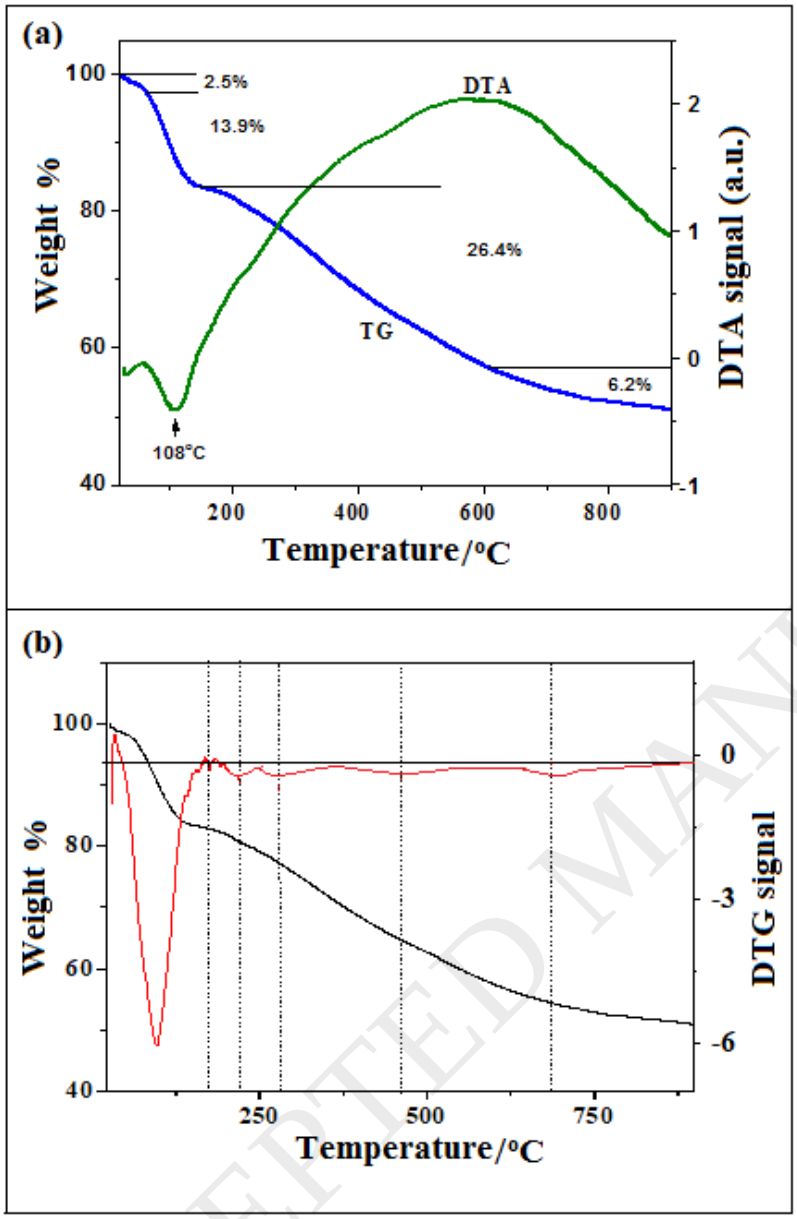

Fig. 2. (a) TG-DTA plot of GBC-120 in nitrogen atmosphere and (b) Comparison of TG/DTG profiles (N_2 atmosphere, heating rate of 10 ^oC min^{-1})

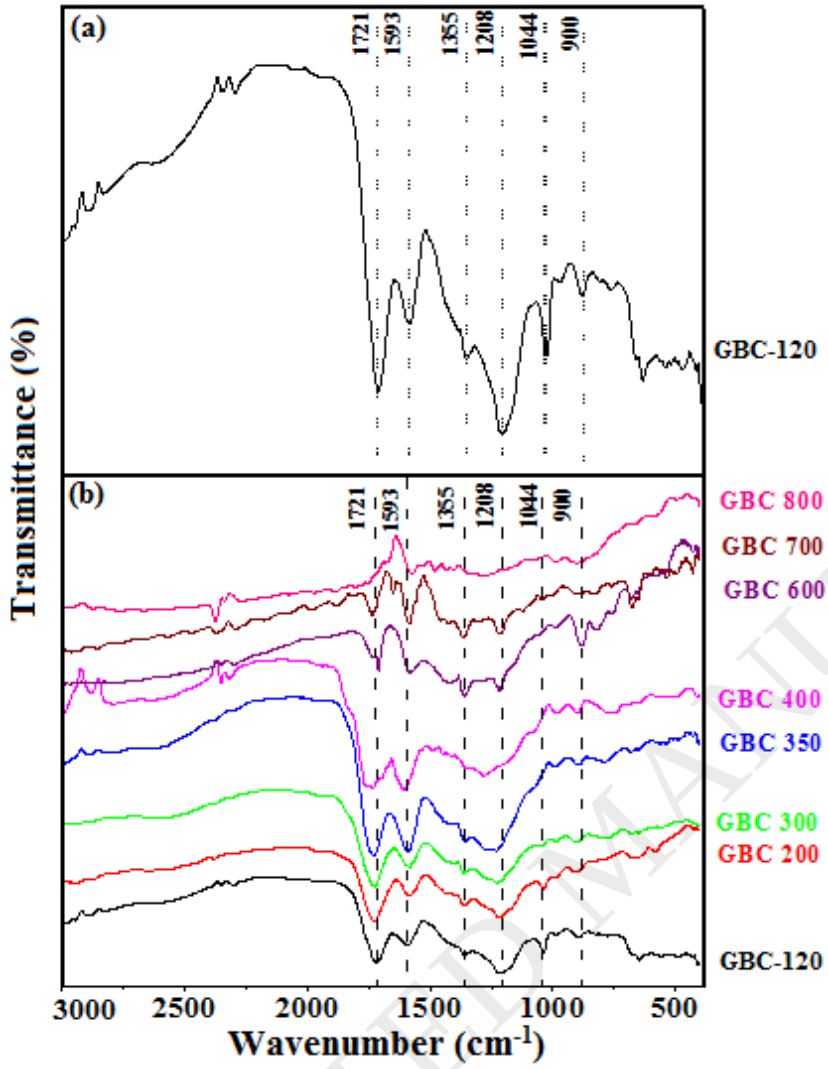

Fig. 3. Infrared spectra of GBC carbons (a) spectrum of GBC-120 (b) spectra of various GBC carbons heat treated between 200 - 800 ^{o}C (using KBr dispersion).

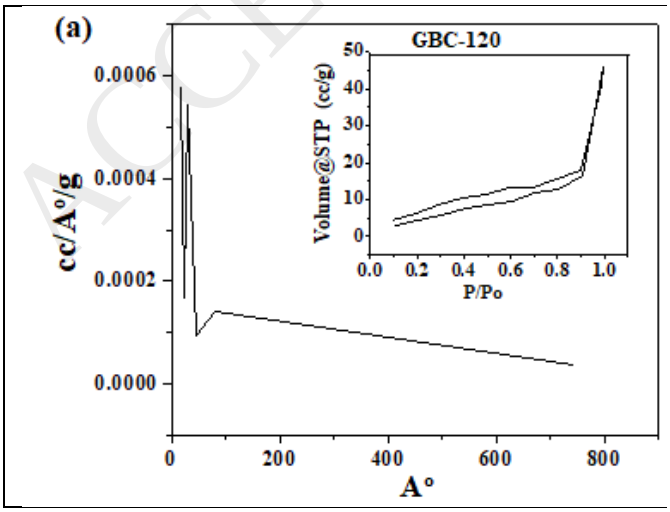

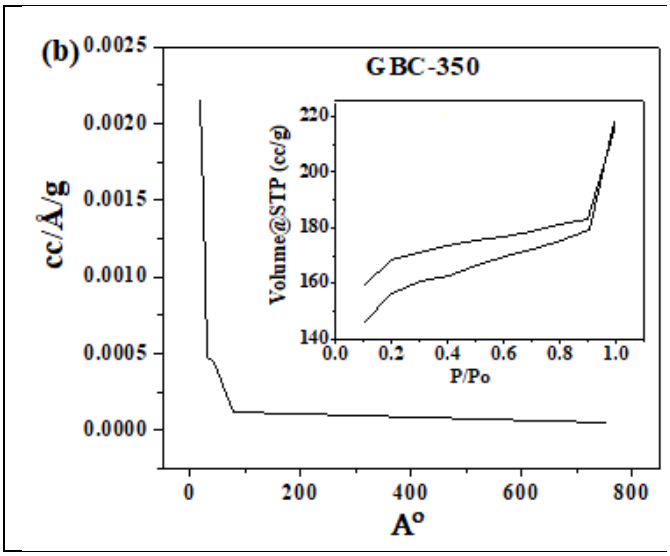

Fig. 4. Pore size distribution and N_2 adsorption-desorption isotherm (inset) for the carbon samples (a) GBC-120 and (b) GBC-350.

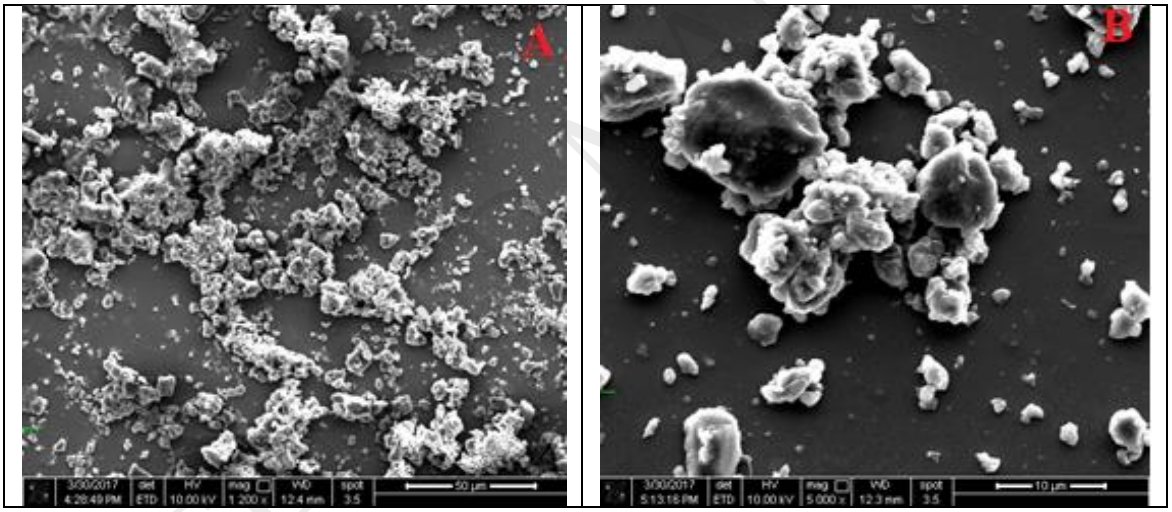

Fig.5. SEM images of (A) GBC-120 (B) GBC-350

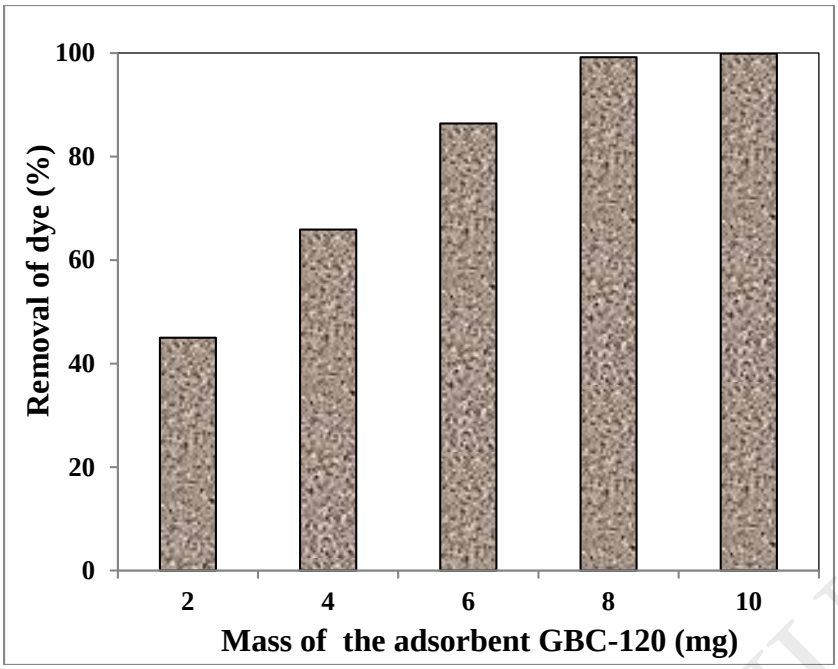

Fig. 6. Effect of amount of adsorbent on adsorption efficiency
Volume of adsorbate: 100 mL, Temperature: 298 K, Contact time: 15 hours, Initial Conc: 25 µg mL^{-1}

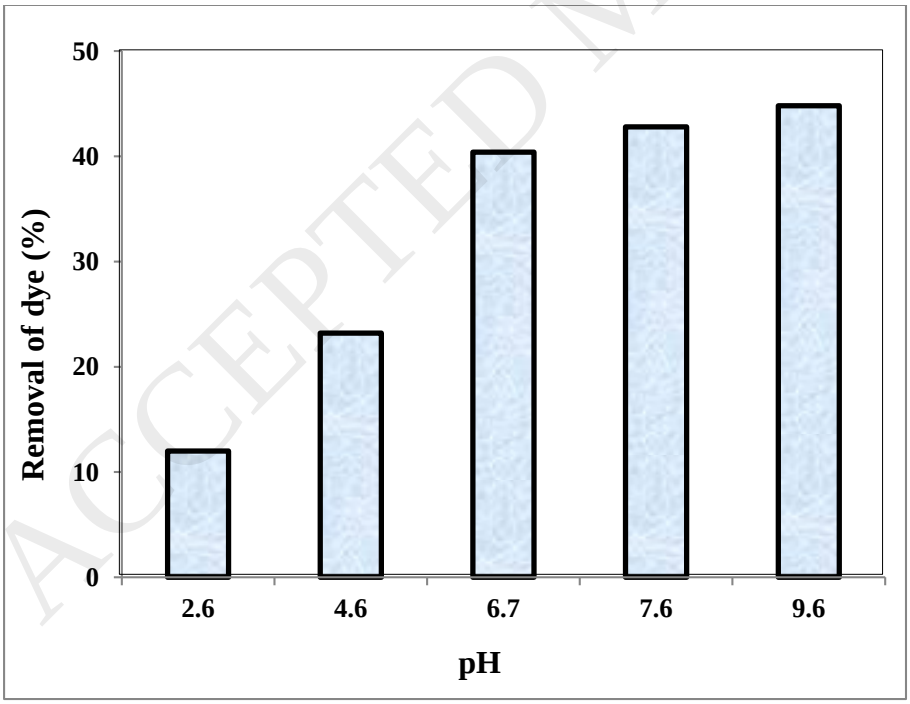

Fig. 7. Relative adsorption efficiency of GBC-120 carbon at different pH values.
Volume of adsorbate: 50 mL, Dosage of adsorbent: 2 mg, Temperature: 298 K, Contact time: 2 hours, Initial Conc: 50 µg mL^{-1}

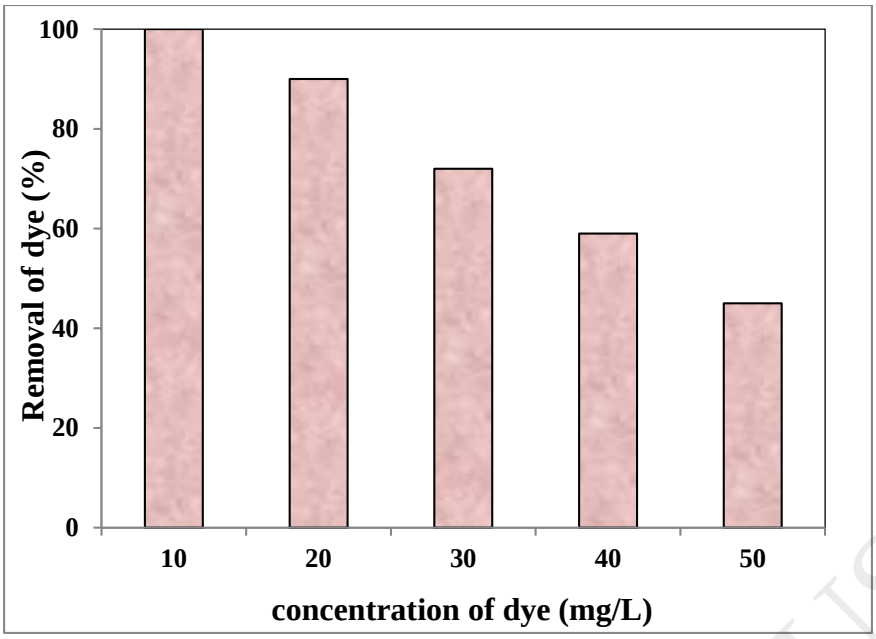

Fig. 8. Effect of intial concentration of methylene blue on adsorption efficiency
Volume of adsorbate: 100 mL, Dosage of adsorbent: 2 mg, pH of the solution: 7.0, Temperature: 298 K, Contact time: 15 hours

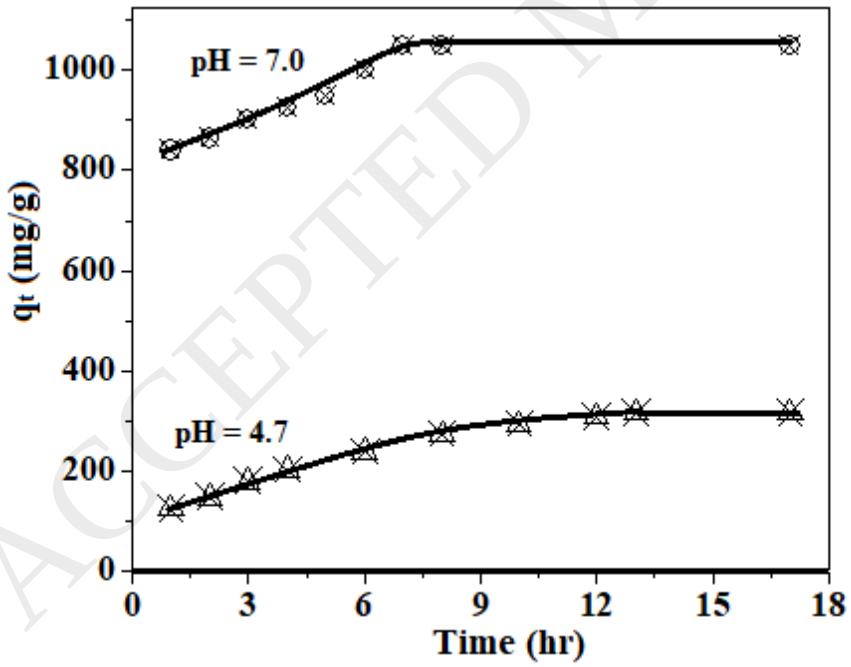

Fig. 9. Kinetic plots obtained when GBC-120 carbon samples were equilibrated with methylene blue solution at pH = 4.7 and 7.0. (q_t is the amounts of dye adsorbed at various time interval t)
Volume of adsorbate: 200 mL, Dosage of adsorbent: 2 mg, Temperature: 298 K, Contact time: 15-20 hours, Initial concentration = 50 µg mL

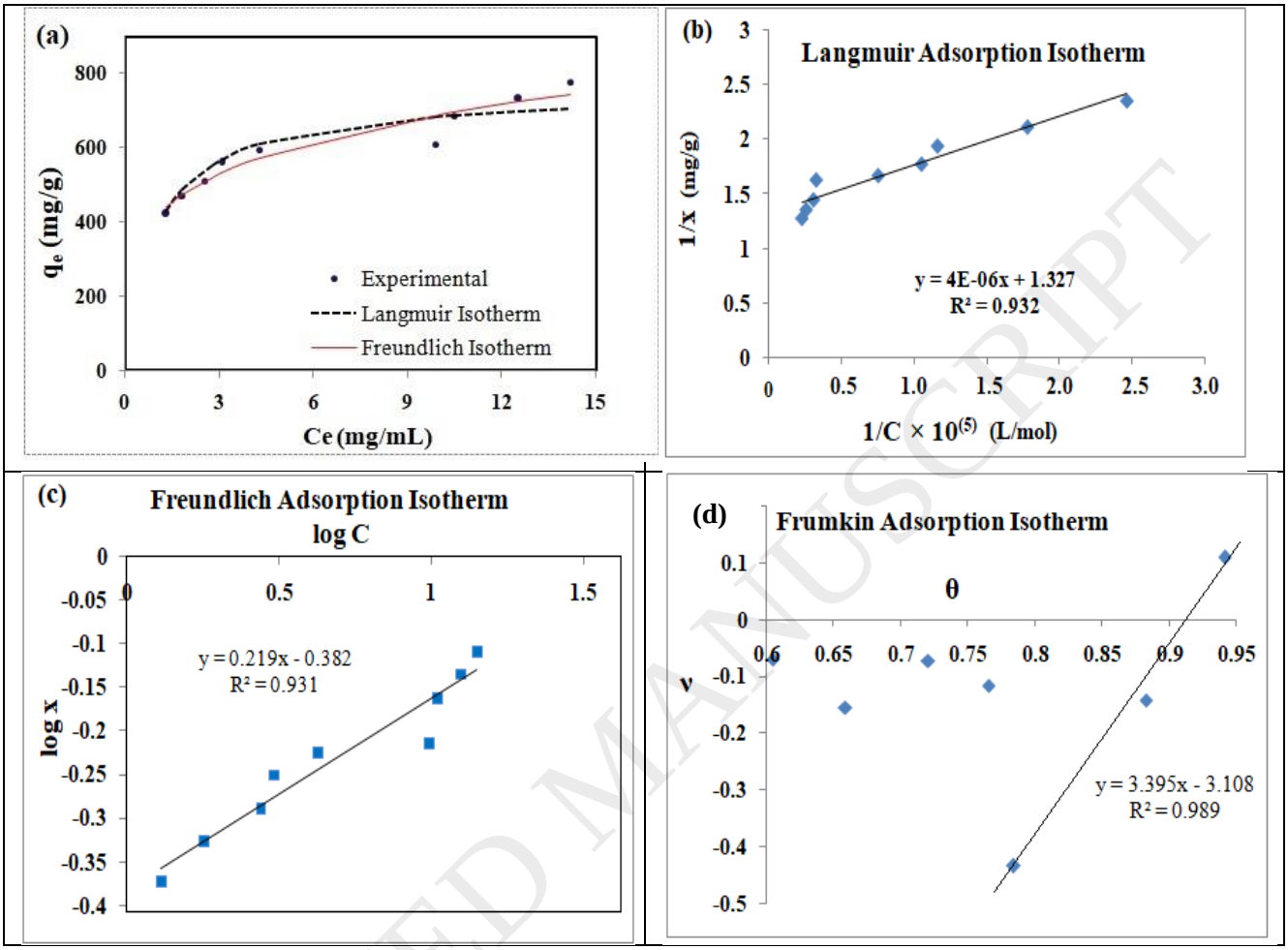

Fig. 10. (a) General adsorption Isotherm and (b-d) Applicability of various adsorption models for adsorption of methylene blue on GBC-120 at 25 ºC and pH=7 .

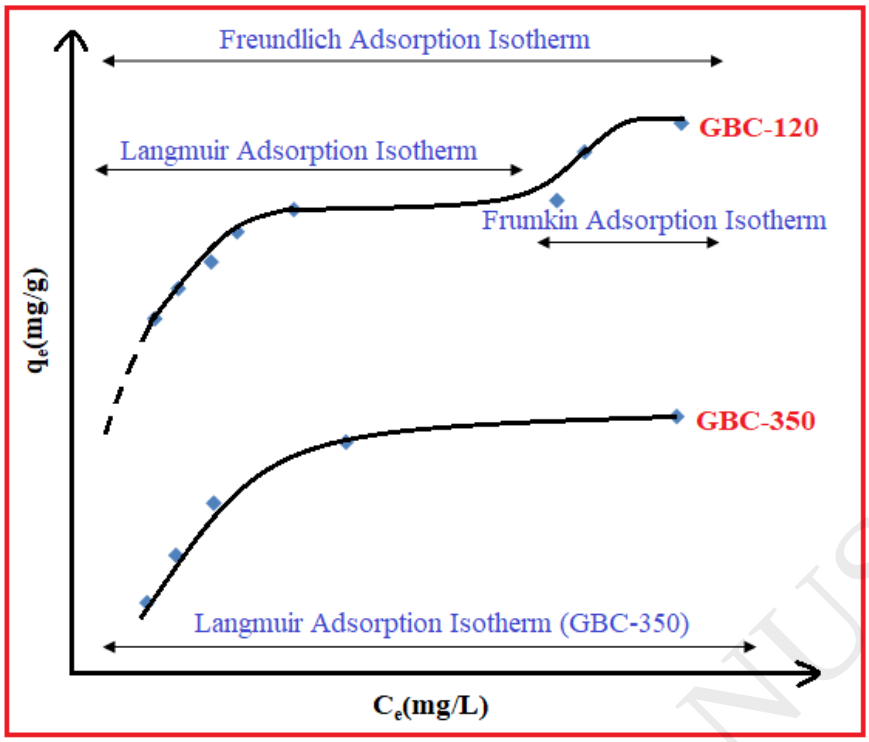

Fig. 11. Summary of the adsorption mechanism discussed in the section 3.3

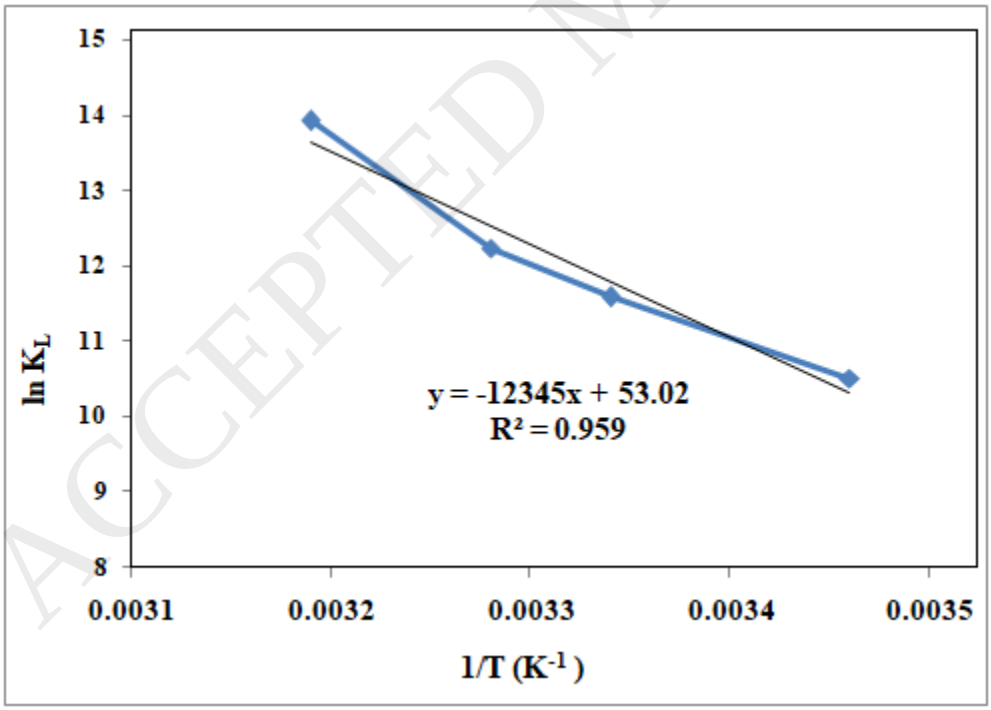

Fig. 12. Plot of ln K_L v/s 1/T for adsorption of methylene blue on GBC-120 at various temperatures between 289 – 323 K.

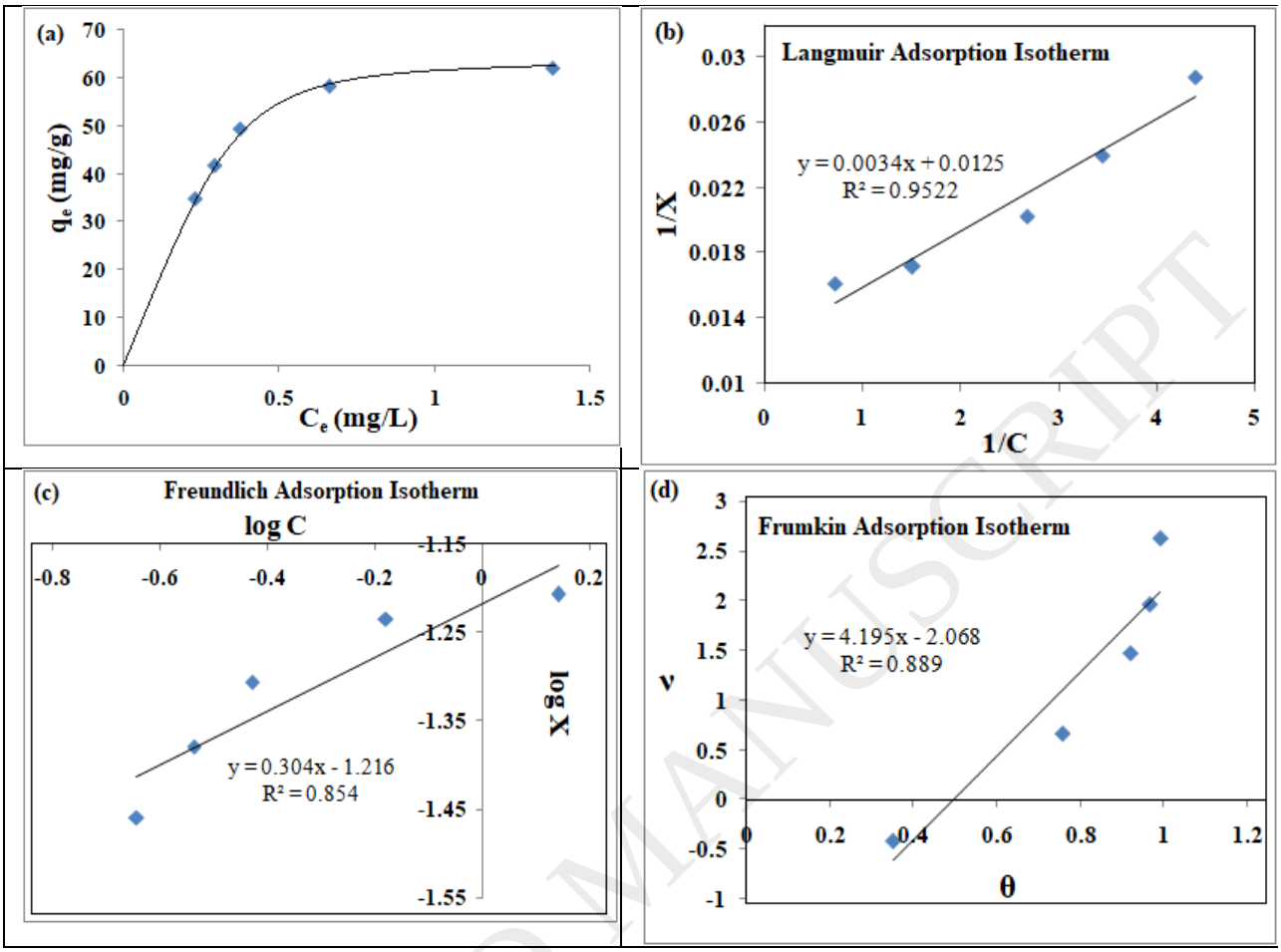

Fig. 13. (a) General adsorption Isotherm and (b-d) Applicability of various adsorption models for adsorption of methylene blue on GBC-350 at 25 ^{o}C.

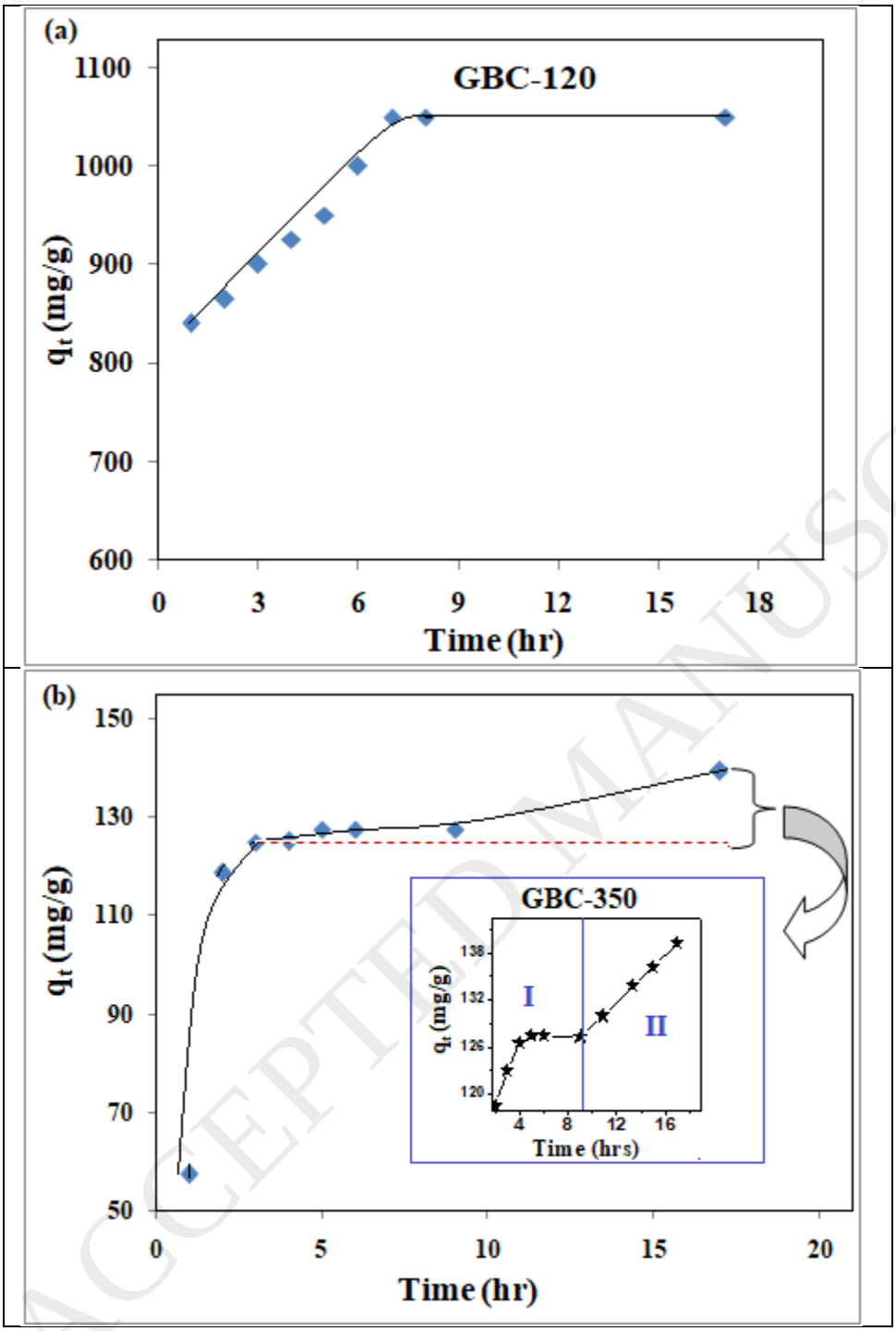

Fig.14. Comparative investigation of adsorption-time behavior of the glycerol based carbons at 25 ^{o}C (a) GBC-120 and (b) GBC-350.

Sample	Pseudo First order Kinetics	Pseudo second order kinetics

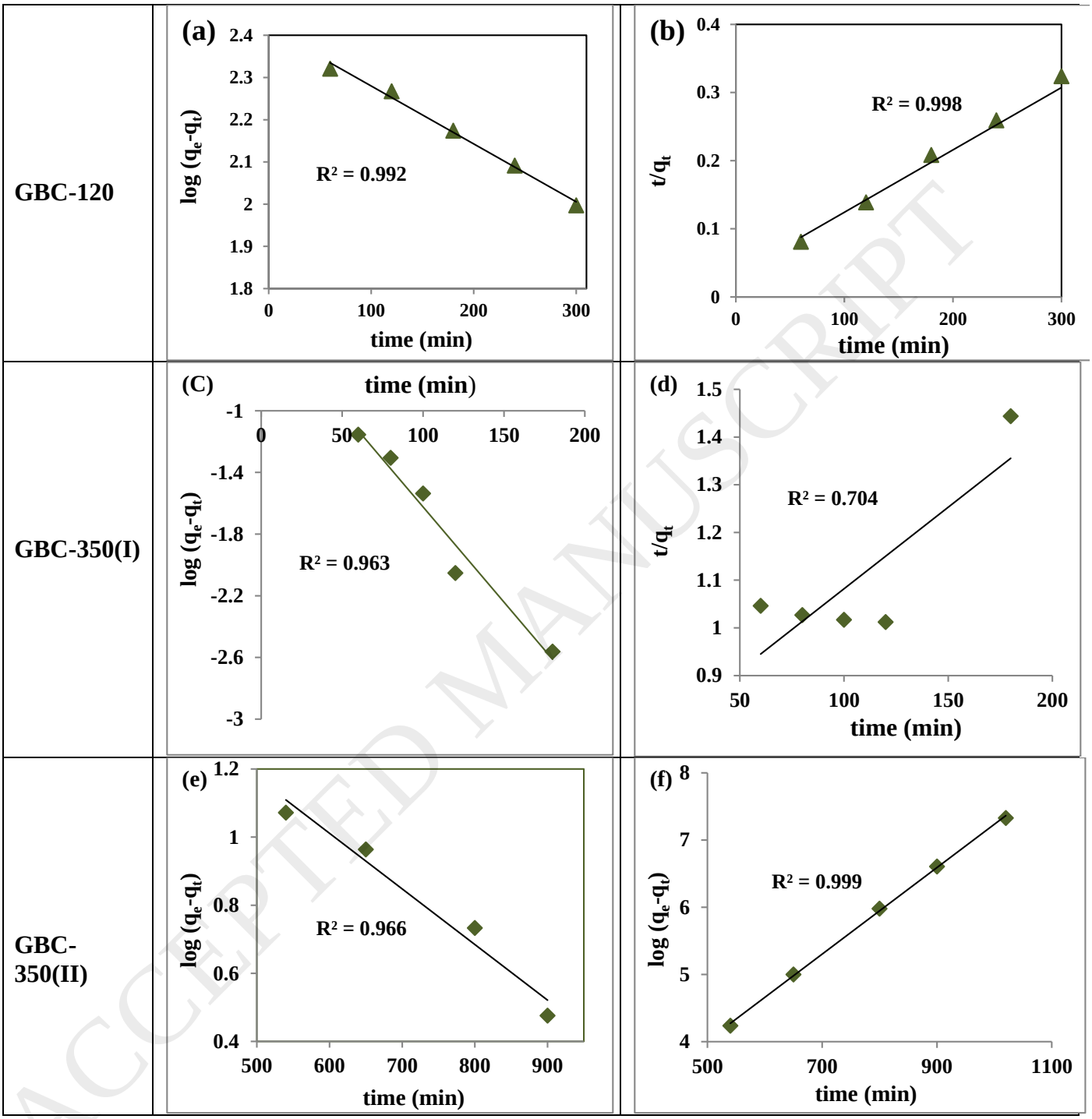

Fig. 15. Application of pseudo first and pseudo second order kinetic models during equilibriation of methylene blue on the GBC samples. GBC-350(I) is initial stage of adsorption and GBC-350(II) is second stage of adsorption.

Table 1: Review of some adsorption and kinetic models

Sr. No.	Adsorption Isotherm	Parameters and their significance
1	Langmuir adsorption isotherm $x = \frac{x_m K c}{1 + Kc}$ $\frac{1}{x} = \frac{1}{x_m K} \cdot \frac{1}{c} + \frac{1}{x_m}$	x = Amount of methylene blue adsorbed per unit mass of carbon (mg g^{-1}). x_m = Maximum adsorption capacity with complete monolayer coverage on the surface of carbon (mg g^{-1}). c = Concentration of methylene blue in the solution which is in equilibrium with the carbon. K = Langmuir adsorption constant which is related to energy of adsorption
2	Freundlich adsorption isotherm $x = k\, c^{\frac{1}{n}}$ $\log x = \log k + \frac{1}{n} \log c$	k = Freundlich adsorption constant which is indicative of maximum adsorption capacity. 1/n = Measure of intensity of adsorption. (1/n = 0 - 1)
3	Frumkin adsorption isotherm $\frac{\Theta}{(1-\Theta)} e^{-2\alpha\Theta} = \frac{\beta}{55.55} c$ $\log\left(\frac{\theta}{(1-\theta)c}\right) = \log\frac{\beta}{55.55} + \frac{2\alpha\theta}{2.303}$ $Where\ \theta = \frac{M}{M_{ads}}$	α = adsorbate interaction parameter β = Adsorption-desorption equilibrium constant. θ = Amount of adsorbate adsorbed at equilibrium. M = Concentration of the dye adsorbed at equilibrium. M_{ads} = Maximum amount of dye adsorbed at equilibrium.
	Kinetic models (expressions in linear form)	
1. 2.	Pseudo first order kinetic model $\log(q_e - q_t) = \log q_e - \frac{K_1}{2.303}\, t$ Pseudo second order kinetic model $\frac{t}{q_t} = \frac{t}{q_e} + \frac{1}{K_2 {q_e}^2}$	K_1 and K_2 are first and second order rate constants. q_e is the amounts of dye adsorbed at equilibrium and q_t is the amounts of dye adsorbed at time t.

Table 2: The assignments corresponding to different frequencies observed in the infra-red spectra of glycerol based carbons.

Frequencies cm^{-1}	**Functional groups**
1721	C = O stretch of COOH and carbonyl group
1593	C = C stretch of graphitic rings
1355	O = S = O stretch of $–SO_3H$
1208	(i) Symmetric S = O stretch (ii) C - OH stretching of phenolic group
1044	Asymmetric stretching of SO_3H

Table 3: The values of surface area, pore volume and pore size of GBC-120 and GBC-350 from BET analysis.

Sample	Surface Area ($m^2\ g^{-1}$)	Pore volume ($cc\ g^{-1}$)	Pore radius (Å)	SEM/ EDAX Analysis Wt (%) of the elements		
				C	O	S
GBC-120	21.00	0.06	18.38	82.45	15.82	1.74
GBC-350	464.00	0.10	18.27	87.55	12.09	0.36

Table 4: Values of various adsorption isotherm parameters during adsorption of methylene blue on GBC-120.

Volume of adsorbate: 100 mL, Dosage of adsorbent: 2 mg, pH of the solution: 7.0, Temperature: 298 K, Contact time: 15 hours					
Langmuir		Freundlich		Frumkin	
X_m (mg/g)	754.00	k (mg/g)	415.00	α (µg/mL)	3.90
K (L/mg)	1.00	1/n	0.22	β (µg/mL)	-172.00
R^2 (Linear)	0.93	R^2 (Linear)	0.93	R^2	0.99
R^2 (Non Linear)	0.84	R^2 (Non Linear)	0.97	--	--

Table 5: Evaluation of thermodynamic parameters during adsorption of methylene blue on GBC-120 at various temperatures.

Volume of adsorbate: 100 mL, Dosage of adsorbent: 2 mg, pH of the solution: 7.0, Contact time: 2 hours										
T (K)	q_e (mg g^{-1})	C_e (µg mL^{-1})	θ_e	K_L (L mg^{-1})	K_L (L mol^{-1}) × 10^5	ln K_L	1/T × 10^3	ΔG (KJ mol^{-1})	ΔH° (KJ mol^{-1})	ΔS° (KJ mol^{-1})
289	265.40	11.70	0.57	0.12	0.37	10.51	3.46	-26.05	102.00	0.44
299	338.00	8.10	0.73	0.33	1.08	11.58	3.34	-28.70		
304	372.20	6.40	0.80	0.65	2.07	12.24	3.28	-30.33		
313	427.80	3.60	0.92	3.48	11.1	13.92	3.19	-34.49		
323	461.90	1.90	1.00	--	--	--	3.09	--		

Table 6: Kinetic parameters obtained from application of pseudo first and pseudo second order kinetic models for adsorption of MB on GBC carbons initial concentration of 50 µg mL^{-1}

Samples	pseudo first order kinetic model			pseudo second order kinetic model			
	R^2	K_1 (min^{-1})	q_e observed (mg g^{-1})	R^2	K_2 (g mg^{-1} min^{-1})	q_e observed (mg g^{-1})	q_e calculated (mg g^{-1})
GBC-120	0.91	0.0046	385	0.99	$4.17*10^{(-5)}$	865	1050
GBC-350 I	0.96	0.0286	408	0.70	$1.56\times10^{(-5)}$	029	130
GBC-350 II	0.97	0.0036	098	**0.99**	$5.14\times10^{(-5)}$	156	139